(Abstract No# 134)

Surface Charging Predictions for Solar Probe Plus

Michelle M. Donegan, Victoria A. Davis, Myron J. Mandell

Abstract— **The spacecraft for the Solar Probe Plus (SPP) mission, with a planned launch of summer 2018, will encounter an extreme near-Sun thermal and plasma environment. It will have a minimum perihelion of 9.86 solar radii (0.0459 AU) and spend over 900 hours within 20 solar radii of the Sun's center. This previously unexplored environment and the unique spacecraft design pose challenges in predicting the degree of surface charging that SPP will experience.**

The purpose of the work presented here is to predict spacecraft surface potentials for a range of environmental conditions in order to guide design choices. The expected plasma environments are specified using a combination of data from HELIOS and modeling results for a range of helioradii from 0.73 AU to SPP's minimum perihelion of 0.0459 AU. Data from HELIOS indicate that a cloud of photoelectrons formed in front of the probe, resulting in distortion of the measured electron distribution below 10-20 eV [1]. More recently, published PIC calculations [2, 3] show that a cylindrical spacecraft can change to negative potentials near the Sun. We present here *Nascap-2k* results for Solar Probe Plus for complex spacecraft geometry and temperature-dependent conductivities and compare those results to those in other studies.

Keywords—surface charging; near-Sun; photoemission

I. INTRODUCTION

A. *The Solar Probe Plus mission*

NASA's Solar Probe Plus (SPP) mission will mark humanity's first visit to our star. Due to launch in the summer of 2018, SPP will orbit the Sun 24 times over a seven-year period. SPP's first perihelion will be at 35.7 solar radii (R_S), and its last three perihelia will be at 9.86 R_S (distances are measured from Sun center); the decreasing perihelia are achieved using gravity assists from 7 Venus flybys. The spacecraft will spend over 900 hours below 20 R_S and over 14 hours below 10 R_S. The SPP science investigations will perform both in situ and remote imaging measurements, obtaining data on the plasma origin, heating, and acceleration of the different solar wind regimes (i.e., slow, fast, and transient solar wind).

The environments that SPP will encounter present unique challenges in designing the spacecraft. Near perihelion, it will experience very high temperatures (up to 1400°C) and extreme solar radiation intensity (up to 475 times that at 1 astronomical unit (AU)). Additionally, the solar wind environment contains large fluxes of charged particles and a distribution of dust particles. This extreme environment begets challenges for thermal and power management, leading to a highly constrained spacecraft design that incorporates electrically insulating surfaces. The spacecraft's reference design at the time of the program's Preliminary Design Review (PDR), held 13-16 January 2014, is shown in Fig. 1.

The need to protect the spacecraft's payload in the near-Sun environment has driven the decision to use a ceramic coating on the Sun-facing Thermal Protection System (TPS). This coating, composed primarily of Al_2O_3 (alumina), is highly refractory and has a low absorptivity-to-emissivity ratio. While it is electrically conductive at the high temperatures expected during SPP perihelia passes and close to conductive for heliocentric distances below 0.25 AU, the coating has high electrical resistivity at the lower temperatures that will be experienced for much of the mission.

The spacecraft also needs to maintain power levels over a range of helioradii, from perihelion out to 1 AU, which has driven the design of the solar arrays. The two arrays are mounted on arms attached to the spacecraft chassis and are moved in and out of the shadow of the TPS (see Fig. 1) in order to maintain constant power levels. Furthermore, the arrays have an active cooling system, which prevents overheating of the solar cell coverglasses and grout. Portions of the solar cell coverglasses therefore have high electrical resistivity.

B. *Spacecraft surface charging*

Spacecraft surface charging is a process in which the currents to and from the spacecraft come into equilibrium. The relevant processes include incoming electrons and ions from the surrounding plasma environment as well as electron- and ion-induced secondary electron emission, backscattered electron emission, and photoemission. This current balance is represented by [4]:

$$J_{net} = \left(J_{inc}^{el} + J_{inc}^{ion}\right) - \left(J_{emit}^{SE} + J_{emit}^{BSE} + J_{emit}^{ion} + J_{emit}^{photo}\right) \quad (1)$$

where J_{net} is the net current, J_{inc}^{el} and J_{inc}^{ion} are the incident electron and ion currents, J_{emit}^{SE} is the current out due to electron-induced secondary electron emission, J_{emit}^{BSE} is the current out due to backscattered electron emission, J_{emit}^{ion} is the current out due to ion-induced secondary electron emission,

Fig. 1. The SPP spacecraft, showing the solar array positions at minimum perihelion (left), 0.25 AU (center), and aphelion (right). The Thermal Protection System (TPS) will be facing the Sun at all times, which provides a shadow cone that protects the payload.

M. Donegan is with the Johns Hopkins University Applied Physics Laboratory, Laurel, 20723, USA (e-mail: michelle.donegan@jhuapl.edu)

V. Davis and M. Mandell are with Leidos, Inc., San Diego, 92121, USA

(Abstract No# 134)

and J_{emit}^{photo} is the current out due to photoemission.

At equilibrium, $J_{net}=0$ and potentials develop on the spacecraft relative to plasma "ground." These potential differences may be either absolute, as when the local spacecraft "ground" charges relative to plasma "ground"; or differential, as when portions of the spacecraft differ from one another in potential.

Electromagnetic cleanness is a prerequisite for space missions, particularly those with in situ instruments. The mission of SPP requires measurement of the key plasma parameters of the near-solar environment, including electric and magnetic fields and the densities and velocity distributions of low-energy solar wind electrons and ions. Charging-induced alterations to the local solar wind electric field could contaminate the measurements of the payload's electric field instrument. Additionally, the disruptions to the local solar wind electric field will influence incident electron and ion trajectories and therefore compromise measurements of those particles. Since these measurements are critical to SPP's science goals [5], it is necessary to understand the degree of surface charging that the spacecraft will experience in the near-solar environment and to use this information to guide the design of the spacecraft. While not a formal requirement, it is strongly preferred that chassis potentials remain within 10 volts (V) of plasma "ground" while the spacecraft is within 0.25 AU from the Sun. The 10 V figure is driven by the mission goal of adequately sampling the solar wind charged particle distribution [5].

While large electrically insulating surfaces are not commonly used in space applications, a modeling study has indicated that it is possible to use them effectively in the near-solar environment, without compromising electric field and low-energy charged particle measurements [6, 7]. Recent studies, however, have also provided a look at the challenges of placing a spacecraft in the near-Sun environment, including the formation of a wake behind the spacecraft and the formation of potential barriers due to photoelectron and secondary electron emission [2, 3, 8, 9].

II. PLASMA ENVIRONMENT

In order to evaluate the surface charging situation for SPP, it was necessary to specify the solar wind environment which it is expected to experience. In particular, nominal values for key fast and slow solar wind parameters and their variations as a function of heliocentric radial distance were required as input for the charging calculations. These parameters include the plasma density n ($n=n_e=n_p$ by quasineutrality for an assumed electron (e) and proton (p) plasma), the bulk flow velocity V, and the electron and proton temperatures T_e and T_p. These parameters result from taking the first three velocity moments of the plasma velocity distribution function, which in the simplest nontrivial case, is well represented by a convected Maxwellian [10]. "Nominal" is taken here to mean the "typical" value of a particular quantity as measured near the ecliptic plane, where that quantity is averaged over a sufficiently long time to smooth out small-scale ($\leq$ day) fluctuations. These parameters provide the input required for modeling surface charging in the solar wind. Since the charging calculations were performed in the local rest frame of the spacecraft, we first transformed all plasma parameters from the sun-centered inertial frame to the spacecraft frame by using the SPP orbit for the closest perihelion pass. Estimates of solar wind parameters that were used to obtain results contained in this report, along with their lower and upper limits, will be described elsewhere [11].

We found from parametric studies that the solar wind parameters that most significantly affect surface charging are the electron temperature and the plasma density associated with the slow and fast solar winds. We have therefore considered a "nominal" solar wind for the fast and slow solar winds over several helioradii as well as variations in electron temperature, ion temperature, and plasma density for selected helioradii. Plasma parameters for "nominal" conditions in the

TABLE I.   SOLAR WIND PARAMETERS VS. HELIORADIUS FOR "NOMINAL" CONDITIONS IN THE FAST SOLAR WIND.

Heliocentric distance (AU)	Electron number density (m^{-3})	Electron temperature (eV)	Proton temperature (eV)	Velocity in x (m/s)	Velocity in z (m/s)	Solar intensity (# of Suns)
0.0459	2.45×10^9	53.1	129.9	-1.95×10^5	-6.72×10^5	475
0.1	3.60×10^8	33.7	81.8	-8.53×10^4	-7.92×10^5	98.3
0.16	1.22×10^8	26.1	63.0	-5.34×10^4	-7.86×10^5	38.6
0.25	4.22×10^7	20.5	49.3	-3.45×10^4	-7.74×10^5	16.1
0.5	8.74×10^6	13.9	33.4	-1.72×10^4	-6.89×10^5	4.00
0.73	3.64×10^6	11.3	27.0	-1.18×10^4	-7.13×10^5	1.88

TABLE II.   SOLAR WIND PARAMETERS VS. HELIORADIUS FOR "NOMINAL" CONDITIONS IN THE SLOW SOLAR WIND.

Heliocentric distance (AU)	Electron number density (m^{-3})	Electron temperature (eV)	Proton temperature (eV)	Velocity in x (m/s)	Velocity in z (m/s)	Solar intensity (# of Suns)
0.0459	1.65×10^{10}	51.9	63.7	-1.95×10^5	-1.91×10^5	475
0.1	2.57×10^9	35.6	31.1	-8.53×10^4	-3.72×10^5	98.3
0.16	9.22×10^8	28.8	20.7	-5.34×10^4	-3.95×10^5	38.6
0.25	3.55×10^8	23.6	14.2	-3.45×10^4	-4.03×10^5	16.1
0.5	7.72×10^7	17.2	7.7	-1.72×10^4	-3.95×10^5	4.00
0.73	3.80×10^7	14.4	5.6	-1.18×10^4	-3.69×10^5	1.88

(Abstract No# 134)

TABLE III.   VARIATIONS OF SOLAR WIND PARAMETERS FROM "NOMINAL" CONDITIONS FOR SELECTED HELIORADII. (PARAMETERS NOT SPECIFIED IN THIS TABLE REMAIN THE SAME AS FOR THE "NOMINAL" CASES.)

Heliocentric distance (AU)	Solar wind type	Variation type	Electron number density (m^{-3})	Electron temperature (eV)	Proton temperature (eV)
0.0459	Fast	Low n, low Te, high Ti	1.23×10^9	48.64	223.14
0.0459	Fast	High n, high Te, low Ti	4.91×10^9	56.89	71.87
0.0459	Slow	Low n, low Te, high Ti	4.13×10^9	45.57	100.04
0.0459	Slow	High n, high Te, low Ti	4.13×10^{10}	59.66	40.51
0.25	Fast	Low n, low Te, high Ti	2.21×10^7	15.7	79.07
0.25	Fast	High n, high Te, low Ti	8.84×10^7	25.02	29.75
0.25	Slow	Low n, low Te, high Ti	8.88×10^7	17.97	22.61
0.25	Slow	High n, high Te, low Ti	8.88×10^8	29.36	8.85

TABLE IV.   SOLAR WIND PARAMETERS FOR "EXTREME" (POST-SHOCK) AND "VERY SLOW" SOLAR WIND CONDITIONS AT MINIMUM PERIHELION. (BOTH CASES HAVE 475 SUNS FOR THE PERIHELION CASE.)

Heliocentric distance (AU)	Variation type	Electron number density (m^{-3})	Electron temperature (eV)	Proton temperature (eV)	Velocity in x (m/s)	Velocity in z (m/s)
0.0459	Extreme	3.30×10^{10}	120.0	3880	-1.95×10^5	-1.00×10^6
0.0459	Very slow	1.65×10^{10}	51.87	63.67	-1.95×10^5	-1.91×10^4

fast and slow solar winds are given in Table I and Table II.

Additionally, plasma parameters for a number of variations on the "nominal" case are shown in Table III, and Table IV gives parameters for an "extreme" (i.e., post-shock) case and a "very slow" solar wind case at minimum perihelion. Although plasma parameters such as solar wind electron temperature and density are generally correlated, we have not treated them as such in constructing our environmental variations.

III.   MODELING

A. Geometric and material model

The *Nascap-2k* spacecraft charging analysis package was used for the modeling in this study, and is described in detail in section IIIB. *Nascap-2k*'s Object Toolkit was used to construct a geometric model of the SPP spacecraft, shown in Fig. 2. The spacecraft includes a ceramic-coated heat shield (TPS) and primary and secondary solar array segments that are progressively stowed within the shadow of the heat shield as the spacecraft approaches the Sun. Within this model, the electrical properties of the materials on the spacecraft's surface are specified. Key material properties (including the bulk conductivity, surface resistivity, secondary electron emission parameters, and photoemission current) were obtained from the literature and from vendor communications. Trajectory-dependent (temperature-dependent) values for conductivity and surface resistivity were used for insulators, since the levels of surface charging (differential as well as relative to plasma "ground") are strongly affected by the conductivity of the insulating materials. Generally the insulator conductivity is highly temperature dependent, and SPP will encounter a wide range of temperatures over the course of its science mission and the orbit as a whole.

Table 5 specifies the major materials used in the SPP model. The heat shield coating is a ceramic mixture of approximately 85% Al$_2$O$_3$, 10% MgO, and 5% BN. This coating will be applied via plasma spray over a conductive barrier layer, which is itself on top of the carbon-carbon composite substrate. The secondary array coverglasses (CMG
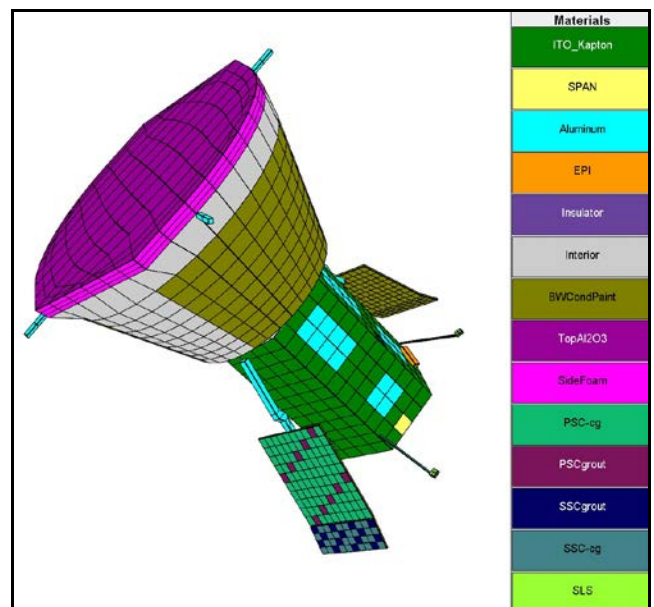

Fig. 2. Geometric model of the SPP spacecraft, as constructed for *Nascap-2k*.

(Abstract No# 134)

TABLE V.   MATERIALS INCLUDED IN THE SPP SPACECRAFT MODEL.

Spacecraft component	Material	Material type
Heat shield coating – top	Al_2O_3/BN/MgO	Insulator
Heat shield sides	Carbon foam	Conductor
Heat shield structure	Carbon-carbon	Conductor
Primary solar array coverglasses	ITO over CMG	Conductor
Secondary solar array coverglasses	AR over CMG	Insulator
Solar array grouting	Conductively coated	Conductor
Spacecraft bus	ITO over Kapton	Conductor
Cooling system radiators	Black/white conductive paint	Conductor
Spacecraft radiators	Aluminum	Conductor

TABLE VI.   BULK CONDUCTIVITIES AND SURFACE RESISTIVITIES OVER A RANGE OF HELIORADII FOR THE HEAT SHIELD COATING..

Helioradius (AU)	Conductivity ($\Omega^{-1}m^{-1}$)	Surface resistivity (Ω/square)
0.0459	Conductive	Conductive
0.1	Conductive	Conductive
0.16	Conductive	Conductive
0.25	6.0×10^{-9}	6.0×10^{11}
0.5	1.0×10^{-15}	1.0×10^{19}
0.73	1.0×10^{-15}	1.0×10^{19}

by Qioptic Space Technology) have a thin layer of MgF_2 serving as an antireflective (AR) coating.

Table 6 shows the bulk conductivities and surface resistivities used for the heat shield coating as a function of helioradius over several points in the SPP orbit. The values for the heat shield coating are those for Al_2O_3 [12] at the expected temperatures. For modeling purposes, conductivities greater than 10^{-9} are taken to be fully conductive. Since an earlier study determined that the results are insensitive to the exact conductivity values, the conductivity of the secondary solar array at closest approach is used for all distances through 0.25 AU.

B. Nascap-2k modeling

For this study, *Nascap-2k* [13, 14, 15] was used to solve Equation 1 for the steady-state spacecraft surface potentials. *Nascap-2k* is a three-dimensional spacecraft-plasma environment analysis computer code developed by Leidos, Inc. with funding from NASA and the Air Force Research Laboratory. It is distributed by NASA's Space Environments and Effects (SEE) Program (http://see.msfc.nasa.gov). *Nascap-2k* charging simulations account for incident plasma currents, secondary and backscattered currents, and photoemission. The three-dimensional code includes the trapping of low energy secondary- and photo-electrons due to barrier formation. In these simulations, the incident plasma currents are taken to be the orbit-limited currents from a hydrogen plasma with both species described by convected Maxwellian distribution functions with the parameters given in Section 2.1. The escaping photocurrent was computed using the spectrum of photoemitted electrons from GEOTAIL as derived in [16].

In magnetospheric and interplanetary space the charge density near a photoemitting surface is dominated by the photoemitted electrons. At 1 AU, the density of photoemitted electrons is ~5×10^8 m^{-3}, compared with typical solar wind density of ~7×10^6 m^{-3}. Both quantities vary approximately as

the inverse square distance from the sun. In the absence of ambient plasma, the photoelectron space charge would cause the potential to decrease without limit as a function of distance from the emitting surface, and all photoelectrons would return to the spacecraft. In reality, there is a distance beyond which the photoelectron space charge density, due to a combination of divergence and loss of returning electrons, is reduced to the order of the ambient density; thus, space charge neutrality is enforced, and photoelectrons with sufficient energy to reach that distance escape the spacecraft. This problem was studied analytically in [17] and more recently, numerically in [3]. A one-dimensional (spherical symmetry) analytic model to determine the extent to which the photocurrent escaping each surface is limited by its space charge was developed for *Nascap-2k* [9]. Qualitatively, this effect is important in the slow solar wind within 0.3 AU, and in the fast solar wind within 0.1 AU for a 1 m spacecraft.

Data from HELIOS indicate that a cloud of photoelectrons formed in front of the probe, resulting in distortion of the measured electron distribution below 10^{-20} eV [1]. More recently, published PIC calculations [2, 3] show that a cylindrical spacecraft can change to negative potentials near the Sun. In addition to the photoemitted electrons, secondary electrons and the deficit of ions in the wake contribute to a space charge barrier surrounding the spacecraft. In these calculations the space charge barrier from the secondary electrons limits the secondary emission resulting in a negative surface potential. An analytic model of the height of the space charge barrier due to secondary electrons was developed for *Nascap-2k* [9]. *Nascap-2k* calculates the barrier height due to photoelectrons, secondary electrons, and the three dimensional geometry, including the deficit of ions in the wake and uses the maximum to limit secondary electron emission. The results presented here make use of this updated code.
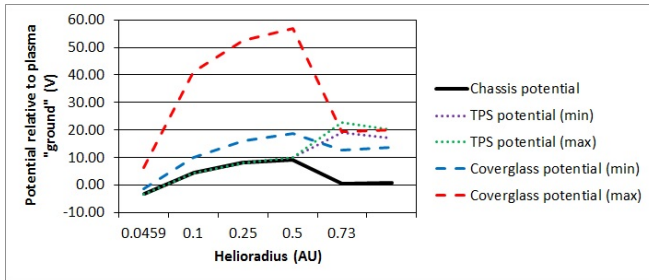
(Abstract No# 134)

Fig. 3. Surface potentials of the chassis, TPS, and secondary array coverglasses relative to plasma "ground" for nominal plasma parameters in the fast solar wind.
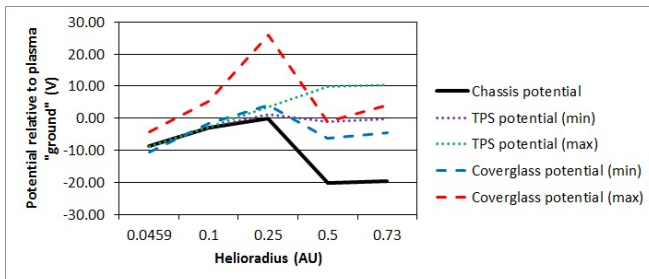

Fig. 4. Surface potentials of the chassis, TPS, and secondary array coverglasses relative to plasma "ground" for nominal plasma parameters in the slow solar wind.

IV. SURFACE CHARGING RESULTS

A. Surface and space potentials

Surface charging results are presented for helioradii ranging from SPP's minimum perihelion of 0.0459 AU to 0.73 AU, for both slow and fast solar wind environments. The results shown here include the photoemission, secondary electron emission, and wake barrier. Surface and space potentials are calculated iteratively.

The TPS and chassis potentials vs. helioradius are plotted in Fig. 3 for the fast solar wind and Fig. 4 for the slow solar wind. As the spacecraft's distance from the Sun increases, the TPS coating becomes less conductive and the TPS and chassis become electrically disconnected from each other, particularly in the slow solar wind environment. Therefore, negative charge that accumulates on the surface of the chassis cannot transfer to the TPS, which, in the slow solar wind, becomes slightly positive due to photoemission. While the potential differences between the TPS and the chassis increase with helioradius, for the parameters used they remain less than 10 V until beyond 0.25 AU. The TPS and chassis potentials relative to plasma "ground" also remain within 10 V until beyond 0.25 AU.

The surface and space potentials in a plane through the center of the spacecraft for the perihelion point in the fast solar wind are graphically illustrated in Fig. 5. Space potentials are dominated by the potential well in the wake, particularly at minimum perihelion. At a Mach number between 2 and 7, the spacecraft travels a few of its own radii before the ions can fill in behind it. The electrons fill in more rapidly. However, the

density to which electrons can accumulate is limited by the space charge of the electrons already in the wake. The Debye length is long enough that the potential well is only about half of the electron temperature.

B. Solar array "shine-through"

The secondary solar array coverglasses become partially conductive near the Sun, which can allow the underlying solar cell potentials to present on the surface – a "shine-through" effect. While this can lead to positive potentials as high as +50 V at the surface, the surface area of the secondary array coverglasses is so small that the effect on the space potentials and on particles is quite small.

The surface potentials are determined by a balance between the net current to the surface and the current conducted through the coverglass. The current through the coverglass is determined by the coverglass conductivity and the differential potential between the surface and the underlying solar cell. "Shine through" occurs when the conductivity is high enough that little differential potential is required to conduct away the net surface flux. Shine through occurs in the intermediate regime (~0.1 to 0.5 AU) where the coverglass conductivity is low and the net surface current moderate. Although conductive materials are preferred on the spacecraft surface, the small areas of non-conductive solar array coverglasses are tolerable in this case.

C. Surface potentials for variations from the "nominal" environment

In order to assess the sensitivity of the surface potentials to the variations in the plasma environment, we also calculated
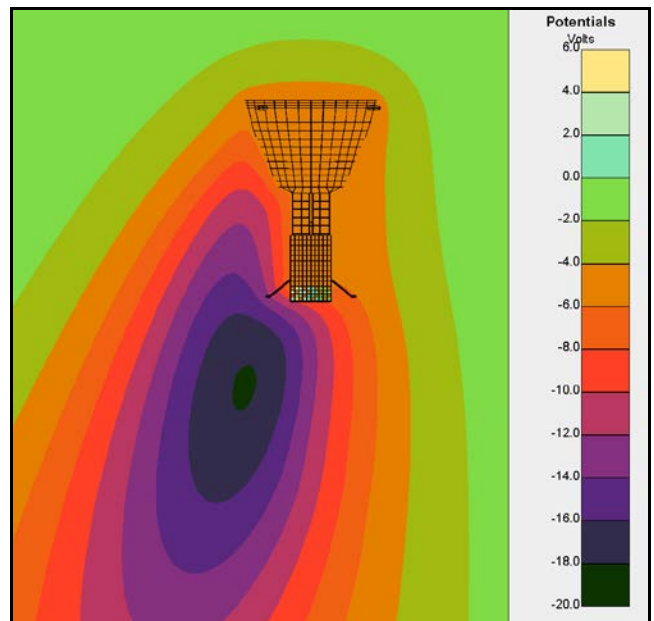

Fig. 5. Surface and space potentials for SPP at perihelion. The Sun-exposed heat shield is conductive and reaches the same potential as the spacecraft chassis. Significant negative potentials occur in the spacecraft wake.

(Abstract No# 134)

TABLE VII.   SURFACE POTENTIALS FOR VARIATIONS OF SOLAR WIND PARAMETERS FROM "NOMINAL" CONDITIONS AT MINIMUM PERIHELION AND 0.25 AU IN THE FAST AND SLOW SOLAR WINDS.

Heliocentric distance (AU)	Solar wind type	Variation type	Chassis potential (V)	Heat shield potential (V)	Coverglass potential (V)
0.0459	Fast	Nominal	-3.3	-3.3	-1.6 to +6.3
0.0459	Fast	Low n, low Te, high Ti	-0.4	-0.4	+2.0 to +18.5
0.0459	Fast	High n, high Te, low Ti	-6.0	-6.0	-5.6 to +0.5
0.0459	Fast	Extreme	-31.1	-31.1	-29.5 to -21.7
0.0459	Slow	Nominal	-8.8	-8.8	-10.5 to -4.2
0.0459	Slow	Low n, low Te, high Ti	-4.7	-4.7	-3.6 to +0.2
0.0459	Slow	High n, high Te, low Ti	-12.6	-12.6	-14.3 to -6.7
0.0459	Slow	Very slow solar wind	-8.6	-8.6	-8.5 to -4.5
0.25	Fast	Nominal	+9.2	+9.8	+18.7 to +56.9
0.25	Fast	Low n, low Te, high Ti	+12.4	+12.8	+22.2 to +61.1
0.25	Fast	High n, high Te, low Ti	+5.0	+5.6 to +6.4	+14.2 to +51.0
0.25	Slow	Nominal	-0.1	+1.1 to +3.5	+4.1 to +25.9
0.25	Slow	Low n, low Te, high Ti	+4.8	+5.4 to +6.2	+13.8 to +50.0
0.25	Slow	High n, high Te, low Ti	-1.2	+1.5 to +3.1	+4.1 to +19.0

charging for the environmental variations described in section II. The conditions that cause the most strongly negative potentials are those for high plasma density, high electron temperature, and low ion temperature. The results of these calculations are shown in Table 7. Table 7 also includes the results for two unusual environments: an "extreme" (post-shock) case and a "very slow solar wind" case. The "extreme" case, with its very high electron temperature, produces the most strongly negative potentials, with the chassis at more than 30 V negative.

In general, the modeling results lead us to expect that SPP will experience potentials in the range -10 V to +10 V. Excursions to -30 V are possible under post-shock conditions. These results are similar in magnitude to those found by the studies in [2] and [3].

V. CONCLUSIONS

We report *Nascap-2k* simulations using Solar Probe Plus geometry and materials and nominal solar wind environments. The chassis potential varies between -10 V and +10 V, with negative potential being more severe in the slow solar wind than in the fast solar wind due to the higher plasma density of the slow solar wind. An extreme shock wave environment predicts a -30 V potential on the chassis; this is primarily due to the higher electron temperature, to which the surface potentials are very sensitive. Under some conditions, underlying solar cell potentials do "shine through" to the secondary solar array surfaces, but the limited surface area means that the effect on space potentials is small.

ACKNOWLEDGMENT

REFERENCES

[1] U. Isensee, "Plasma disturbances caused by the Helios spacecraft in the solar wind," J. Geophys., vol. 42, p. 581, 1977.

[2] S. Guillemant, V. Genot, J.C. Mateo-Velez, R. Ergun, and P. Louarn, "Solar wind plasma interaction with Solar Probe Plus spacecraft," Ann. Geophys. Vol. 30, p. 1075, 2012.

[3] R. E. Ergun, D. M. Malaspina, S. D. Bale, J. P. McFadden, D. E. Larson, F. S. Mozer, N. Meyer-Vernet, M. Maksimovie, P. J. Kellogg, and J. R. Wygant, "Spacecraft charging and ion wake formation in the near-Sun environment," Phys. Plasma, vol. 17, p. 1134, 2010.

[4] E. C. Whipple, "Potentials of surfaces in space," Rep. Prog. Phys., vol. 44, p. 1197, 1981.

[5] NASA (2008), "Solar Probe+: science objectives and measurement requirements," Solar Probe Plus: report of the Science and Technology Definition Team, NASA/TM—2008–214161, 2008.

[6] M. M. Donegan, J. L. Sample, J. R. Dennison, and R. Hoffmann, "Spacecraft coating-induced charging: a materials and modeling study of environmental extremes," AIAA Journal of Spacecraft and Rockets, vol. 47, no. 1, pp. 134-146, 2010.

[7] M. M. Donegan, R. B. Decker, N. Raouafi, D. Lario, and P. N. Bernasconi, "Surface charging analyses for the Solar Probe Plus mission," 11th Spacecraft Charging Technology Conference, Albuquerque, NM, 2010.

[8] M. J. Mandell, V. A. Davis, G. T. Davis, R. H. Maurer, and C. Herrmann, "Photoemission driven charging in tenuous plasma," IEEE Trans. Plasma Sci., vol. 40, p. 209, 2012.

[9] M. J. Mandell, V. A. Davis, and M. M. Donegan, "Analytic model for space charge limiting of photoemission in near-Sun environments," 13th Spacecraft Charging Technology Conference, Pasadena, CA, 23-27 June 2014.

(Abstract No# 134)

[10] F. Scherb, "Velocity distributions of the interplanetary plasma detected by Explorer 10," Space Research, vol. 4, p. 797, 1964.

[11] M. M. Donegan, V. A. Davis, M. J. Mandell, R. B. Decker, and N. Raouafi, " Spacecraft surface charging modeling for Solar Probe Plus: environmental estimates and charging results for a mission to the near-Sun environment," unpublished, 2014.

[12] R. Morrell, "Handbook of Properties of Technical and Engineering Ceramics, Part 2: Data Reviews; Section I: High-Alumina Ceramics," Her Majesty's Stationery Office, London, pp. 1–255, 1987.

[13] M. J. Mandell, V. A. Davis, and D. L. Cooke, "*Nascap-2k* spacecraft charging code overview," IEEE Trans. Plasma Sci., vol. 34, no. 5, p. 2084, 2006.

[14] V. A. Davis and M. J. Mandell, "*Nascap-2k* Scientific Documentation for Version 4.1," AFRL,-RV-PS-TR-2011-0089, Vol II, 2011.

[15] V. A. Davis and M. J. Mandell, "*Nascap-2k* Scientific Documentation for Version 4.2," unpublished, 2014.

[16] T. Nakagawa, T. Ishii, K. Tsuruda, H. Hayakawa, and T. Mukai, "Net current density of photoelectrons emitted from the surface of the GEOTAIL spacecraft," Earth Planets and Space, vol. 52, pp. 283-292, 2000.

[17] R. L. Guernsey and J. H. M. Fu, "Potential Distribution Surrounding a Photo-Emitting Plate in a Dilute Plasma," J. Geophys. Res., vol. 75, p. 3193, 1970.